

High Stiffness of Human Digital Flexor Tendons Is Suited for Precise Finger Positional Control

Samuel R. Ward, Gregory J. Loren, Scott Lundberg, and Richard L. Lieber

Departments of Radiology Orthopedic Surgery and Bioengineering, Biomedical Sciences Graduate Group, University of California and Veterans Administration Medical Centers, San Diego, California

Submitted 15 March 2006; accepted in final form 8 July 2006

Ward, Samuel R., Gregory J. Loren, Scott Lundberg, and Richard L. Lieber. High stiffness of human digital flexor tendons is suited for precise finger positional control. *J Neurophysiol* 96: 2815–2818, 2006. First published July 26, 2006; doi:10.1152/jn.00284.2006. The objective of this study was to define the biomechanical properties of the human digital flexor tendons and to compare these biomechanical properties to other muscle-tendon units in the forearm. Mechanical measurements were performed on fresh-frozen tendons under physiological load and temperature conditions. Loads were determined by first measuring the physiological cross-sectional area of each digital belly of the flexor digitorum superficialis (FDS) and flexor digitorum profundus (FDP) and estimating maximum tension (P_o) of that specific muscle head. Loading each tendon to the appropriate P_o resulted in no significant difference in tendon strain among any of the tendons within each muscle ($P > 0.05$; digits 2–5) or between muscle types (FDP vs. FDS). The one exception to this finding was that a significantly higher strain at P_o was observed in the FDP tendon to the small finger ($P < 0.05$). Average absolute strains observed for the FDP and FDS tendons ($1.20 \pm 0.38\%$, mean \pm SD; $n = 39$) were significantly lower than those observed previously in a study of the prime movers of the wrist. The measured strain of $\sim 1.5\%$ was less than half of that predicted to occur in muscles of this architectural design. Modeling sarcomere shortening magnitudes during FDP or FDS contraction yielded a value of only $0.10 \mu\text{m}$, which would have a negligible effect on the force generating capacity of these muscles. Thus the high stiffness of the digital flexor tendons suits them well for fine positional control and would render their muscle spindles quite sensitive to length perturbations at the fingertips.

INTRODUCTION

The control of movement by the neuromuscular system requires coordination between the physiological properties of the neural activation system and the biomechanical properties of the muscle-tendon unit. All muscle actions are “interpreted” by the tendinous material that is placed in series with the muscle. As such, significant tendon compliance may have a profound effect on the muscle’s ability to control movement or to sense joint position. Although the biomechanical properties of isolated tendon specimens have been studied in some detail (Butler et al. 1978), only recently have muscle-tendon interactions been characterized under physiological conditions (Buchanan et al. 2001; De Zee et al. 2000; Lieber et al. 2000). These “physiologically relevant” biomechanical studies have demonstrated that tendons are more than inert connectors between muscles and bones, rather their mechanical properties

are customized to provide specializations that enable certain muscle-tendon units to accomplish a particular task. In a previous study, it was found that tendon compliance measured under physiological loads (from 0 up to maximum tetanic tension, i.e., P_o) of the prime movers of the wrist was not a constant (Loren and Lieber 1995). Indeed strain at P_o was significantly different among tendons with the largest strain observed in the flexor carpi ulnaris (FCU, $3.68 \pm 0.31\%$) and the smallest strain observed in the extensor carpi radialis longus (ECRL, $1.78 \pm 0.14\%$). Further, strain magnitude was significantly positively correlated with the tendon length-to-fiber length ratio of the muscle-tendon unit, a measure of the intrinsic compliance of the muscle-tendon unit (Zajac 1989). We interpreted these data to indicate that muscle-tendon units show remarkable specialization and that tendon intrinsic properties accentuated the muscle architectural specialization.

The architectural characteristics of the digital flexors are well suited for performing high-excursion, low-force movements given their relatively long fibers and small physiological cross-sectional areas (Lieber et al. 1992b). Because fine digital manipulation requires precise control of fingertip position, we hypothesized that the stiffness of digital flexor tendons was high because energy storage and muscle injury would not drive the adaptation of these tendons. Thus to test this hypothesis, we measured tendon strain in each tendon of the human flexor digitorum superficialis and profundus (FDS and FDP) by loading them through the range of forces predicted to be generated by their associated muscles rather than simply performing traditional elongation-to-failure experiments on isolated FDP and FDS tendons.

METHODS

Muscle architecture was determined according to the methods previously implemented (Lieber et al. 1990). Five fresh-frozen cadaveric specimens were used, intact from the midhumeral level and free of obvious musculoskeletal defects. The flexor digitorum superficialis (FDS) and flexor digitorum profundus (FDP) from five specimens were isolated by careful dissection of the forearm. The muscle-tendon units ($n = 40$) were removed and weighed. After division at the musculotendinous junction, muscles were fixed for architectural measurements and tendons remained unfixed for materials testing. This experimental protocol was approved by the Anatomical Services Department at the University of California San Diego.

Muscle length (L_m) was measured as the distance from the origin of the most proximal muscle fibers to the insertion of the most distal

Address for reprint requests and other correspondence: R. L. Lieber, Dept. of Orthopaedics, U.C. San Diego School of Medicine and V.A. Medical Center, 3350 La Jolla Village Dr., La Jolla, CA 92093-9151 (E-mail: rlieber@ucsd.edu).

The costs of publication of this article were defrayed in part by the payment of page charges. The article must therefore be hereby marked “advertisement” in accordance with 18 U.S.C. Section 1734 solely to indicate this fact.

muscle fibers. Then, using the $L_f:L_m$ ratios previously measured in our laboratory (Lieber et al. 1992b), muscle fiber length was calculated for each specimen (L_f). Surface pennation angle (θ) with the muscle under zero tension was also used from the previous study. Muscle length and fiber length were normalized to an optimal sarcomere length of 2.5 μm (Lieber et al. 1994) using laser diffraction of fiber specimens to compensate for variations in limb position that may occur during fixation.

Muscle physiological cross-sectional area (PCSA) was determined according to the equation previously described (Sacks and Roy 1982)

$$\text{PCSA}(\text{cm}^2) = \frac{\text{muscle mass (g)} \cdot \cos\theta}{\rho(\text{g/cm}^3) \cdot \text{fiber length (cm)}} \quad (1)$$

where ρ = muscle density (1.056 g/cm^3) (Mendez and Keys 1960). Based on the fact that muscle PCSA predicts muscle maximum tetanic tension (P_o), P_o for each muscle was predicted from architectural measurements by multiplying calculated PCSA by a muscle specific tension of 22.5 N/cm^2 (Close 1972; Powell et al. 1984), and this force was used for each tendon as its maximal loading value.

Physiological tendon loading

Thawed tendon lengths of the FDS and FDP muscles for digits 2, 3, 4, or 5 or the index, long, ring, and small fingers were measured with digital calipers to the nearest 0.1 mm. Using elastin stain, transverse dye lines were applied to the unloaded central tendon region at a 20-mm gauge length. The tendon was placed in a 37°C saline bath, and clamped to the arm of a dual-mode servo-motor (Model 310B, Cambridge Technology, Watertown, MA), permitting controlled loading. The free end of tendon was secured to a stationary clamp yielding ~60 mm of exposed tendons between clamps.

The motor was driven in five linear ramp load-unload cycles to the P_o of the individual musculotendinous actuator tested. To minimize strain rate effects, load was imparted relatively slowly over a 30-s interval (0.017 Hz) and released over a consecutive period using a D/A signal generated by the SuperScope software (version 2.0, GW Instruments, Somerville, MA). Actual strain rates ranged from 0.05 to 0.14%/s. This rate variation was due to the length variability of the specimens themselves. Simultaneous force-time records were obtained at 0.1-s intervals via the servo-motor interfaced with a micro-computer (Apple Computer, Cupertino, CA). A video camera with macro lens recorded dye line spacing during loading for subsequent strain analysis. The fourth load-deformation cycle was utilized for strain analysis using a video dimension analyzer (VDA; Model 303, Physiological Instruments in Medicine, San Diego, CA). The VDA signal was amplified by a factor of 100 and low-pass filtered at 10 Hz (universal amplifier 13-4615-58, Gould, Cleveland, OH) prior to computer acquisition. Each specimen was strain-tracked three times from parallel regions of the tendon specimen with corresponding records averaged over time. From corresponding points on the load- and strain-time relationships, the load-strain curve was constructed.

Tendon area was assessed by volumetric displacement of 0.9% NaCl solution at room temperature placed in a graduated cylinder etched at 0.1-ml increments. Initial volume was recorded at the base of the meniscus to the nearest 0.05 ml. The tendon specimen was submerged in the cylinder after gentle blotting with gauze and the final volume recorded. Three displacement measurements were made, divided by specimen length, and averaged to yield mean tendon CSA. This method had previously been shown to be more accurate than microscopic planimetry of tendon sections or point counting of multiple sections (Loren and Lieber 1995).

To predict the magnitude of muscle sarcomere shortening that occurred at the expense of tendon lengthening during a maximal muscle contraction or the amount of joint rotation resulting from finger loading, the theoretical model previously described was used (Lieber et al. 1992a). Briefly, this model assumes that sarcomere

length-tension and force-velocity properties are identical among muscles and uniform across the entire muscle. The model also assumes a finite time course of cross-bridge attachment (Huxley 1957), an ideal sarcomere length-tension relationship (Gordon et al. 1966), an ideal force-velocity relationship (Edman 1979; Katz 1939), and uniform aponeurosis and external tendon material properties. The model was implemented as previously described with the appropriate modifications made for differences in filament length between frogs and humans and tendon mechanical properties were specifically modified for each specimen.

Biomechanical parameters for individual tendon samples were analyzed by two-way ANOVA using muscle type (FDP vs. FDS) and digit (2, 3, 4, or 5) as grouping variables. Multiple paired comparisons among tendons were performed post hoc using Fisher's protected least-squares difference method. Data were analyzed using StatView 4.5 software (Abacus Concepts, Berkeley, CA). Significance level (α) was selected as 0.05; statistical power ($1 - \beta$) exceeded 80% for all parameters for which differences were not significant. Data are expressed as means \pm SE unless otherwise noted. Exponential curves for the individual load-strain and stress-strain relationships were obtained in the form $y = a \cdot e^{bx}$ with correlation coefficients exceeding 0.70 for all data sets.

RESULTS

As expected based on gross inspection of the muscles and tendons, the FDS to the small finger was significantly less massive (3.55 ± 0.80 g; $P < 0.005$), had a significantly lower predicted maximum tetanic tension (P_o ; 9.31 ± 1.73 N; $P < 0.005$), and had a significantly shorter (182.6 ± 9.2 mm; $P < 0.01$) and thinner (4.04 ± 0.83 mm²; $P < 0.001$) tendon compared with the other extrinsic finger flexors (Table 1). In addition, it was noted that the tendons of the FDP muscles as a whole were significantly longer (278.9 ± 30.8 mm; $P < 0.001$) and had significantly greater CSA (12.03 ± 2.9 mm²; $P < 0.001$) compared with those attached to the FDS muscles (8.60 ± 3.32 mm²; $P < 0.001$). No significant differences were noted in measured sarcomere length (L_s) or in tendon length to fiber length ratio ($L_t:L_f$) among muscle-tendon units.

Under physiological loads, the relationship between load and strain was characterized by a curve with progressively increasing slope and no clear demarcation between toe and linear regions as is evident in traditional deformation-to-failure experiments. At P_o , no significant difference was noted in observed stress or strain across either muscle groups or digits ($P > 0.5$, with the exception being the higher strain noted in the FDP tendon to the small finger, Fig. 1). This uniformity existed despite the observed differences in tendon length, tendon CSA, P_o , and L_f noted in the previous section and reveals the ability of tendons to adapt material properties so as to maintain consistent strains (Table 1).

Simulation of an isometric contraction was used to predict the maximal sarcomere shortening allowed at the expense of tendon lengthening, given the observed properties of each muscle-tendon unit. As displayed in Table 1, all of these values fell near or below 0.1 μm (range: 0.051–0.111 μm ; mean: 0.088 ± 0.019 μm). Given myosin and actin filaments length of 1.65 and 1.3 μm , respectively (Lieber et al. 1994), L_s changes of this magnitude would produce muscle force changes of <5% of P_o .

TABLE 1. Anatomical and biomechanical properties of muscle-tendon units ($n = 5/\text{specimen}$)

	Flexor Digitorum Profundus				Flexor Digitorum Superficialis				Two-Way ANOVA P Value		
	2	3	4	5	2	3	4	5	By muscle	By digit	Crossover
Muscle mass, g	16.86 ± 3.86	23.00 ± 4.96	16.86 ± 3.64	19.92 ± 4.29	21.24 ± 4.78	28.34 ± 6.38	17.72 ± 4.00	*3.55 ± 0.80	>0.5	<0.05	>0.05
L_f , mm	94.66 ± 3.93	96.56 ± 0.56	95.72 ± 3.49	80.79 ± 3.53	96.39 ± 8.70	90.87 ± 7.55	88.53 ± 13.42	72.26 ± 8.79	>0.1	>0.05	>0.5
PCSA, cm ²	1.74 ± 0.44	2.24 ± 0.49	1.68 ± 0.39	2.27 ± 0.43	2.17 ± 0.53	3.08 ± 0.78	1.99 ± 0.43	*0.41 ± 0.77	>0.5	>0.05	<0.05
P_o , N	39.15 ± 9.98	50.54 ± 10.97	37.80 ± 8.87	51.14 ± 9.65	48.75 ± 11.86	69.27 ± 17.66	44.72 ± 9.61	*9.31 ± 1.73	>0.5	>0.05	<0.05
L_t , mm	292.6 ± 7.1	309.00 ± 9.7	272.8 ± 8.3	241.20 ± 7.1	229.0 ± 11.8	264.6 ± 9.6	257.8 ± 5.2	*182.6 ± 9.2	<0.0001	<0.0001	<0.05
$L_t:L_f$	3.12 ± 0.19	3.20 ± 0.10	2.85 ± 0.13	3.00 ± 0.09	2.48 ± 0.32	3.00 ± 0.30	3.16 ± 0.41	2.64 ± 0.34	>0.1	>0.5	>0.1
L_s , μm	2.26 ± 0.69	2.34 ± 0.05	2.28 ± 0.08	2.41 ± 0.07	2.47 ± 0.09	2.41 ± 0.08	2.46 ± 0.15	2.30 ± 0.12	>0.1	>0.5	>0.1
Tendon CSA, mm ²	11.40 ± 0.97	14.44 ± 1.00	13.42 ± 0.91	8.84 ± 0.76	8.36 ± 0.61	11.54 ± 0.97	10.46 ± 0.46	*4.04 ± 0.83	<0.0001	<0.0001	>0.5
Stress at P_o , MPa	3.42 ± 0.79	3.39 ± 0.54	2.71 ± 0.47	5.74 ± 0.86	5.59 ± 1.03	6.51 ± 2.02	4.24 ± 0.83	*2.14 ± 0.35	>0.1	>0.1	<0.05
Strain at P_o , %	1.16 ± 0.13	1.00 ± 0.04	1.21 ± 0.12	1.53 ± 0.06	0.83 ± 0.04	1.42 ± 0.09	1.21 ± 0.07	*0.98 ± 0.04	>0.05	<0.05	<0.0001
ΔL_s at P_o , μm	0.090	0.07	0.08	0.111	0.051	0.103	0.092	0.065	>0.05	>0.05	>0.05

Data are presented as means ± SE. L_f , normalized fiber length; PCSA, physiological cross sectional area; P_o , estimated maximum isometric tension; L_t , tendon length; L_s , sarcomere length; CSA, cross-sectional area; ΔL_s at P_o , change in sarcomere length at maximum predicted tension. *, significant difference between FDS and FDP at a specific digit. Bold type denotes significant difference.

DISCUSSION

The purpose of this investigation was to define tendon strain at predicted physiologic loads in the extrinsic digital flexors of the human hand. In so doing, we hoped to further understand the role of tendon compliance in digital function and to compare these properties with the function of other muscle-tendon units (MTUs) in the upper extremity. In Loren and Lieber's study of wrist tendons, MTUs with $L_t:L_f$ in the range representative of typical digital flexor specimens (3.0–3.5) were predicted to have tendon compliance in the range of ~2.5% strain at P_o based on the equation relating $L_t:L_f$ and strain at P_o in the wrist movers. We found the digital flexor tendons to be significantly stiffer than predicted by that model with strain at P_o ranging from 0.70 to 1.69% for individual specimens (mean $1.20 \pm 0.38\%$, Fig. 2), thus implying a different functional goal (Fig. 2). This very low compliance corresponded to a very low L_s shortening during maximal isometric contraction, on the order of 0.1 μm , in contrast to

much larger values in the 0.5- to 0.7- μm range for the wrist movers. Conversely, then, one may also state that tendon length would vary little during flexion or extension movements of the finger, thus making muscle (and fiber) length highly dependent on fingertip position.

Extrinsic digital flexors serve a dual function in the human hand, serving to powerfully flex the DIP and PIP joints and participate in the maintenance of high grip force in conjunction with interosseus- and lumbrical-mediated flexion of the MCP joint. In addition, as the sole flexors of the interphalangeal joints, they serve as the most proximate determinants of fingertip position across a variety of MCP and wrist joint positions (Ranney 1995). How this fine control, critical to many manipulative tasks, is achieved has been the subject of investigation by others with the focus falling on two primary pathways, one starting with the interphalangeal and MCP joint proprioceptive afferents, the other with the muscle spindles present within the digital flexors themselves. In 1997, (Kilbreath et al. 1997) reported that a digital nerve block at the level of the MCP joint, while nullifying the input from the finger joint proprioceptors, did not diminish the ability of normal volunteers to control fingertip position despite wide ranges in the level of force being applied to the pads of the

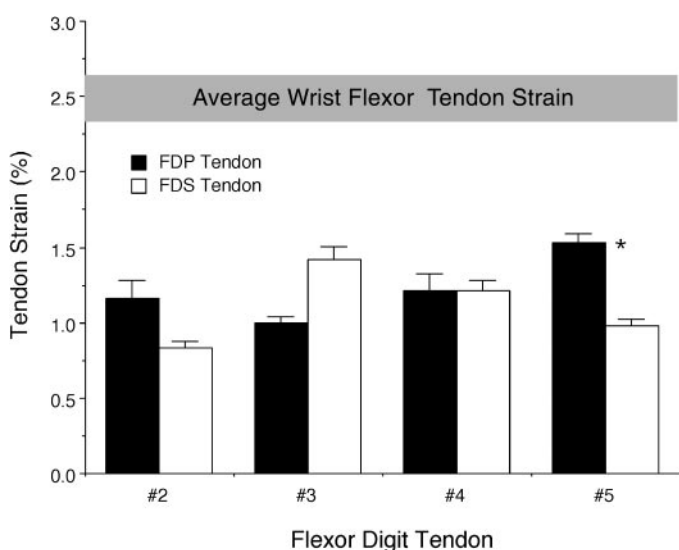


FIG. 1. Comparison of the strain at P_o in the flexor digitorum superficialis and profundus (FDS and FDP) tendons. There were no significant differences in strain between these 2 muscles, except at the 5th digit. Both muscles had significantly lower tendon strain compared with muscles at the wrist (see text for details). Abscissa numbers correspond to digit number and values are means ± SE; *, $P < 0.05$.

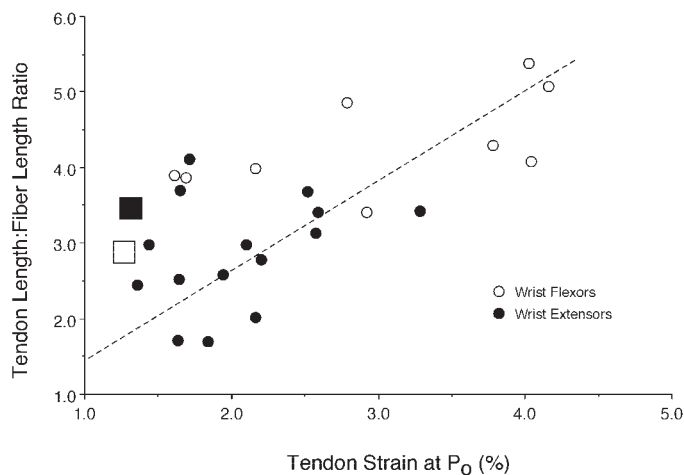


FIG. 2. Scatter plot of tendon strain at P_o (ordinate) vs. tendon length: fiber length ratio (abscissa) for muscles of the wrist (●, extensors; ○, flexors) and finger flexors (■, FDP; □, FDS). These values are significantly more stiff compared with the prime movers of the wrist.

fingers. This finding highlights the important role of intramuscular (muscle spindle) afferents in the active control of fingertip position and in the setting of various forces antagonizing interphalangeal flexion. We postulate that this function is served in the human hand, in part, by minimizing any muscle spindle length change that does not reflect change in fingertip position (that is, changes in L_s caused by stretching of the attached tendon).

There are several potential limitations to this study. First, there are data suggesting that the freeze-thaw process tends to reduce the elastic modulus of human tendon (Clavert et al. 2001; Smith et al. 1996). Those experiments, however, were performed under load-to-failure conditions, whereas our data were obtained within the physiologic loading range. The process of matching the loading capacity of an individual muscle head to its respective tendon requires the use of cadaveric tissue, so there is no alternative to this testing paradigm. Experimentally, any alteration in material properties from the in vivo state would be systematic across tendons and therefore would not change our results. Second, the external tendon and aponeurosis were modeled as a single unit with a single set of material properties. There are published data suggesting both that the aponeurosis and external tendon *do* have different material properties (Kawakami and Lieber 2000) or *do not* have different material properties under isometric conditions (Roeleveld et al. 1993). However, it is clear aponeurosis compliance should be measured during an active muscle contraction (Lieber et al. 2000) where it is considerably stiffer compared with passive conditions, and this is not possible under these experimental conditions. Finally, modeling the aponeurosis and external tendon together facilitated comparisons with previous data collected in the wrist. Nevertheless, as future studies resolve the complexities of anisotropic tendon material properties and the shear loads they impose on muscle fibers, this would be an interesting model consideration at the wrist and hand.

In conclusion, the biomechanical properties of human extrinsic digital flexor tendons are well suited to the functional task of precise positional fingertip control. The higher stiffness of these tendons may be an important parameter to consider in the modeling of human hand and finger function as well as an important consideration in the choice of flexor tendon repair or replacement materials and the design of flexor tendon reconstruction surgeries.

ACKNOWLEDGMENTS

The authors acknowledge S. Enguidanos for technical assistance on the experimental measurements.

GRANTS

This work was supported by the National Institutes of Health Grants AR-40539 and HD-044822 and the Department of Veterans Affairs.

REFERENCES

- Buchanan C, Marsh R, De Zee M, Bojsen-Moller F, and Voigt M.** Effects of long-term exercise on the biomechanical properties of the Achilles tendon of guinea fowl. *J Appl Physiol* 90: 164–171, 2001.
- Butler DL, Grood ES, Noyes FR, and Zernicke RF (Editors).** Biomechanics of ligaments and tendons. *Exer Sport Sci Rev* 6: 125–181, 1978.
- Clavert P, Kempf JF, Bonomet F, Boutemy P, Marcelin L, and Kahn JL.** Effects of freezing/thawing on the biomechanical properties of human tendons. *Surg Radiol Anat* 23: 259–262, 2001.
- Close RI.** Dynamic properties of mammalian skeletal muscles. *Physiol Rev* 52: 129–197, 1972.
- De Zee M, Bojsen-Moller F, and Voigt M.** Dynamic viscoelastic behavior of lower extremity tendons during simulated running. *J Appl Physiol* 89: 1352–1359, 2000.
- Edman K.** The velocity of unloaded shortening and its relation to sarcomere length and isometric force in vertebrate muscle fibers. *J Physiol* 246: 255–275, 1979.
- Gordon AM, Huxley AF, and Julian FJ.** The variation in isometric tension with sarcomere length in vertebrate muscle fibers. *J Physiol* 184: 170–192, 1966.
- Huxley AF.** Muscle structure and theories of contraction. *Prog Biophys Mol Biol* 7: 255–318, 1957.
- Katz B.** The relation between force and speed in muscular contraction. *J Physiol* 96: 45–64, 1939.
- Kawakami Y and Lieber RL.** Interaction between series compliance and sarcomere kinetics determines internal sarcomere shortening during fixed-end contraction. *J Biomech* 33: 1249–1255, 2000.
- Kilbreath S, Refshauge K, and Gandevia S.** Differential control of the digits of the human hand: evidence from digital anesthesia and weight matching. *Exp Brain Res* 117: 507–511, 1997.
- Lieber RL, Brown CG, and Trestik CL.** Model of muscle-tendon interaction during frog semitendinosus fixed-end contractions. *J Biomech* 25: 421–428, 1992a.
- Lieber RL, Fazeli BM, and Botte MJ.** Architecture of selected wrist flexor and extensor muscles. *J Hand Surg* 15A: 244–250, 1990.
- Lieber RL, Jacobson MD, Fazeli BM, Abrams RA, and Botte MJ.** Architecture of selected muscles of the arm and forearm: anatomy and implications for tendon transfer. *J Hand Surg* 17A: 787–798, 1992b.
- Lieber RL, Leonard M, and Brown-Maupin C.** Muscle contraction effects on aponeurosis and tendon load-strain properties. *Cells Tissues Organs* 166: 48–54, 2000.
- Lieber RL, Loren GJ, and Fridén J.** In vivo measurement of human wrist extensor muscle sarcomere length changes. *J Neurophysiol* 71: 874–881, 1994.
- Loren GJ and Lieber RL.** Tendon biomechanical properties enhance human wrist muscle specialization. *J Biomechan* 28: 791–799, 1995.
- Mendez J and Keys A.** Density and composition of mammalian muscle. *Metabolism* 9: 184–188, 1960.
- Powell PL, Roy RR, Kanim P, Bello M, and Edgerton VR.** Predictability of skeletal muscle tension from architectural determinations in guinea pig hindlimbs. *J Appl Physiol* 57: 1715–1721, 1984.
- Ranney D.** The hand as a concept: digital differences and their importance. *Clin Anat* 8: 281–287, 1995.
- Roeleveld K, Baratta RV, Solomonow M, van Soest AG, and Huijij PA.** Role of tendon properties on the dynamic performance of different isometric muscles. *J Appl Physiol* 74: 1348–1355, 1993.
- Sacks RD and Roy RR.** Architecture of the hindlimb muscles of cats: functional significance. *J Morphol* 173: 185–195, 1982.
- Smith CW, Young IS, and Kearney JN.** Mechanical properties of tendons: changes with sterilization and preservation. *J Biomech Eng* 118: 56–61, 1996.
- Zajac FE.** Muscle and tendon: properties, models, scaling, and application to biomechanics and motor control. *Crit Rev Biomed Eng* 17: 359–411, 1989.